J. Am. Soc. Mass Spectrom. (2012)
DOI: 10.1007/s13361-012-0453-4

RESEARCH ARTICLE

The Use of MALDI-TOF-MS and *In Silico* Studies for Determination of Antimicrobial Peptides' Affinity to Bacterial Cells

Santi M. Mandal,[2] Ludovico Migliolo,[1] Octavio L. Franco[1]

[1]Centro de Analises Proteômicas e Bioquímicas, Programa de Pós-Graduação em Ciências Genômicas e Biotecnologia, UCB, Brasília, Brazil
[2]Mass Spectrometry and Proteomics Laboratory Central Research Facility, Indian Institute of Technology Kharagpur, Kharagpur, 721302 WB, India

Abstract

Several methods have been proposed for determining the binding affinity of antimicrobial peptides (AMPs) to bacterial cells. Here the utilization of MALDI-TOF-MS was proposed as a reliable and efficient method for high throughput AMP screening. The major advantage of the technique consists of finding AMPs that are selective and specific to a wide range of Gram-negative and -positive bacteria, providing a simple reliable screening tool to determine the potential candidates for broad spectrum antimicrobial drugs. As a prototype, *amp-1* and *-2* were used, showing highest activity toward Gram-negative and -positive membranes respectively. In addition, *in silico* molecular docking studies with both peptides were carried out for the membranes. *In silico* results indicated that both peptides presented affinity for DPPG and DPPE phospholipids, constructed in order to emulate an in vivo membrane bilayer. As a result, *amp-1* showed a higher complementary surface for Gram-negative while *amp-2* showed higher affinity to Gram-positive membranes, corroborating MS analyses. In summary, results here obtained suggested that *in vitro* methodology using MALDI-TOF-MS in addition to theoretical studies may be able to improve AMP screening quality.

Key words: Affinity constant, Antimicrobial peptides screening, Molecular modeling, MALDI-TOF-MS

Introduction

In recent years, antimicrobial resistance has become a serious problem that threatens the continued effectiveness of traditionally used antibiotics [1]. There is a crucial need to find new antimicrobials that overcome the ineffectiveness of traditional antibiotics. Antimicrobial peptides (AMPs) are of wide interest as they are rapid-acting and provide exceptionally promising alternatives. It is widely accepted that the primary target of AMPs is the cell membrane of bacteria, normally acting by pore formation. Nevertheless, AMPs may also act on bacterial membranes by different mechanisms, either in translocation and interaction with intracellular targets or by membrane permeabilization itself [2, 3]. Moreover, the selectivity and specificity of most AMPs to bacterial membrane are important determinants of their antimicrobial activities [4].

The interactions of AMPs with various model lipid systems have been examined using several methods, such as, ^{1}H nuclear magnetic resonance (NMR), capillary electrophoresis, UV spectroscopy, microcalorimetry and fluorescence techniques as well SPR, QCM, and solid-state NMR, in order to determine the binding specificity [4–6]. Otherwise, a few studies have used mass spectrometry soft ionization,

Electronic supplementary material The online version of this article (doi:10.1007/s13361-012-0453-4) contains supplementary material, which is available to authorized users.

Correspondence to: Octavio L. Franco; *e-mail:* ocfranco@gmail.com

Published online: 25 August 2012

Received: 27 April 2012
Revised: 28 June 2012
Accepted: 18 July 2012

commonly facilitating the detection of small molecules that weakly bond or non-covalently attach with biomacromolecules. Van De Kerk-Van Hoof and Heck [7] demonstrated the effectiveness of ESI-MS to evaluate the binding affinities of several glycopeptide antibiotics with a range of receptor-mimicking peptides. MALDI TOF MS has some advantage over ESI TOF MS for biomacromolecule analyses, particularly in whole cell bacterial characterization [8].

In the present study, MALDI TOF MS is used for rapid screening for evaluation of the binding affinity of two AMPs to the bacterial cell. The first one, a synthetic cyclic Trp-rich antimicrobial peptide [9], Cys-Ala-Trp-Leu-Trp-Ala-Cys named *amp-1*, was used as prototype to study the interactions with bacterial membranes [10]. Furthermore, Cys-Val-Glu-Iso-Lys-Lys-Iso-Phe-His-Asp-Asn, commercially known as bacitracin and here named *amp-2*, was also evaluated [11]. Theoretical docking studies were also performed in order to better understand the MS analyses obtained. For this, *in silico* Gram-negative and -positive bacterial membranes were constructed. Peptides were docked to membranes and lipid affinity theorized in order to better understand how both peptides select and further interact with the membranes.

Material and Methods

Solid-Phase Peptide Synthesis

For the study, the Trp-rich antimicrobial peptide *amp-1* was synthesized by stepwise solid-phase using the *N*-9-fluorenylmethyloxycarbonyl (Fmoc) strategy with a Rink amide resin (0.52 mmol.g^{-1}) [12]. Side chain protecting groups t-butyl for threonine and (triphenyl)methyl for histidine were added. Couplings were performed with 1,3-diisopropylcarbodiimide/1-hydroxybenzotriazole (DIC/HOBt) in *N,N*-dimethylformamide (DMF) for 60 to 120 min. Fmoc deprotections (15 min, twice) were conducted with 4-methylpiperidine:DMF solution (1:4; by volume). Cleavage from the resin and final deprotection of side chains were performed with TFA:water:1,2-ethanedithiol (EDT): triisopropylsilane (TIS), 94.0:2.5:2.5:1.0, by volume, at room temperature for 90 min. After this, the crude product was precipitated with cold diisopropyl ether and 200 mL aqueous acetonitrile at 50 % (by volume). The extracted peptide was twice freeze-dried for purification. Amino acid derivatives and other reagents for solid-phase peptide synthesis were obtained from Merck-NovaBiochem (Whitehouse Station, NJ, USA), Peptides International (Louisville, KY, USA), or Sigma-Aldrich (St. Louis, MO, USA). The bacitracin, known here as *amp-2* peptide, was purchased from Sigma-Aldrich (CAS Number: 1405-87-4).

Peptide Purification

The purity peptide degree here utilized for all experiments was ≥95 %. The *amp*-1 crude peptide was solubilized in 0.1 % trifluoroacetic acid (TFA) and filtered with a Millex filter 0.22 μm 25 mm (Millipore-Merck, Billerica, MA, USA). The crude extract was submitted to semi-preparative RP-HPLC C18 NST (5 μm, 250×10 mm) chromatography using the following mobile phase conditions: H_2O:ACN:TFA (95:05:0.1, vol:vol:vol) for 5 min, than a linear gradient to H_2O:ACN:TFA (05:95:0.1, vol:vol:vol) for 60 min at a flow rate of 2.5 mL.min^{-1}. The experiments were conducted at room temperature and monitored at 216 nm. Fractions were manually collected and lyophilized. The synthetic peptide concentrations for all *in vitro* experiments were carried out by using the measurement described by Murphy and Kies [13] with ABS_{205}, ABS_{215}, and ABS_{225} nm. The quantification to *amp-1* and *amp-2* was calculated for all *in vitro* experiments through the molar extinction coefficient using ProtParam tools found in the Swiss-Prot database (www.expasy.org).

Mass Spectrometry Analyses

Amp-1 and *amp-2* molecular masses were performed by using a Voyager DE Pro MALDI mass spectrometer equipped with 337 nm N_2 laser (Applied Biosystems, Framingham, MA, USA). Major peak protein was dissolved in α-cyano-4-hydroxycinnamic acid matrix solution (1:3, vol/vol), spotted onto a MALDI target massive plate and dried at room temperature for 15 min. Peptide monoisotopic mass was obtained in reflector mode with external calibration, performed using calibration mixture 1 (Applied Biosystems) -Arg1-Bradykinin (*m/z*, 904.468), Angiotensin I (*m/z*, 1296.685), Glu1-fibrinopeptide B (*m/z*, 1570.677), and ACTH (18-39) (*m/z*, 2465.199). Spectra reproducibility was five times checked from separately spotted samples.

In Vitro Affinity Assay

A stock solution (1 mM) was prepared and stored at 4±2 °C. Different concentrations (20–100 μM) of *amp-1* and *amp-2* were incubated with *Staphylococcus epidermidis* NCIM2493 (Gram-positive) and *Escherichia coli* ATCC25922 (Gram-negative) at 30 °C for 30 min. Bacterial concentration was kept at 2×10^5 cells per mL and final reaction volume was 100 μL. After incubation, cells were twice washed with 50 mM phosphate saline buffer, pH 6.4, and centrifuged at 10,000 rpm for 3 min. Then 50 μL of 80 % acetonitrile containing 0.1 % TFA was added to the bacterial pellet and vigorously mixed for 10 min. The supernatant was collected after centrifugation at 10,000 rpm in Eppendorf centrifuge (5415D) for 5 min designated as Sample 1. The residual pellet was resuspended in 50 μL of 80 % acetonitrile containing 0.1 % TFA and vigorously mixed for lyses the cells, being designated as Sample 2. To perform MALDI MS analysis, five μL of each sample was mixed with 5 μL of MALDI matrix, α-cyano-4-hydroxycinnamic acid (10 mg/mL) and 2 μL of the mixture was spotted onto a MALDI stainless steel plate. The MALDI mass spectrometer

equipped with 337 nm N_2 laser (Applied Biosystems) was used and the spectra were recorded in the positive ion linear mode in accelerating voltage 20 kV.

Affinity Binding Constant Calculation

Affinity binding constants (K) of AMPs were calculated from the ratio of the intercept on the vertical coordinate axis to the slope obtained for each peptide. The plot of $1/[(AMP)_0–(AMP)_f]$ versus 1/L, where $(AMP)_0$ is the initial mass spectra intensity of AMP and $(AMP)_f$ is the recorded integrated intensity [intensity of *amp* obtained from Sample 1 + intensity of *amp* obtained from Sample 2 at different *amp* concentrations (L) incubated with bacterial cell.

Molecular Modeling

The three-dimensional models for *amp-1* and *amp-2* were constructed based on the structures of 1h5o and 1p68 PDB code, which presented 57 % and 46 % of identity, respectively. The pdb code structure 1h5o, named crotamine, was used as the template for *amp-1*. This is an antimicrobial peptide component of the snake venom from *Crotalus durissus terrificus*, which belongs to the myotoxin protein family [14]. The pdb code structure 1p68, which was used as the template for *amp-2*, is named S-824 and is a four-helix bundle domain from *Escherichia coli* obtained through a combinatorial library of de novo amino acid sequences [15]. Two hundred theoretical tridimensional peptide structures were constructed using Modeller v. 9.8 for each peptide [16]. The *amp-1* was constructed with N- and C-terminus linked by disulfide bond. Otherwise, after construction of the *amp-2* model some modifications and minimizations were done by YASARA software based on the molecular formula for bacitracin from *Bacillus licheniformis* obtained in the Sigma-Aldrich home page - CAS Number: 1405-87-4 (Figure 1). The *amp-1* and *amp-2* final models (i.e., geometry, stereochemistry, and energy distributions in the models, were evaluated using PROSA II to analyze packing and solvent exposure characteristics and PROCHECK for additional analysis of stereochemical quality [17]. In addition, RMSD was calculated by overlap of Cα traces and backbones onto the template structure through the program 3DSS [18]. The peptide structures were visualized and analyzed on Delano Scientific's PYMOL [19] http://pymol.sourceforge.net/. To calculate the grand average of hydropathicity, named GRAVY, ProtParam was used, which is a tool that allows the analysis computation of various physical-chemical parameters for a given amino acid sequence [20].

In Silico Membrane Interactions

All docking calculations were performed using AUTODOCK 4.2 program [21]. Docking simulation of both peptides (*amp-1* and *amp-2*) was performed toward two membranes (Gram-negative and Gram-positive). The membranes were constructed by using the CHARMM-GUI server [22], and the composition for each membrane was in accordance with Lohner et al. [23]. For Gram-negative membranes a proportion of 9:1 between two types of anionic lipids, phosphatidylethanolamine (DPPE) and phosphatidylglycerol (DPPG), was used. For Gram-positive membrane only DPPG was used. The ratios of peptide to lipid molecules for both analyses with Gram-positive and -negative were of 1 with studies of molecular dynamics realized by Pimthon and co-workers [24]. All hydrogen atoms were added using the Auto-Dock Tool. Grid maps were calculated with 35×35×15 and 30×30×20 points for *amp-1* and *amp-2*, respectively, and 1.0 Å spacing centered on the membrane surface, allowing interaction with all head groups exposed. In order to understand the *in vitro* results a membrane system was constructed with reduced size, showing a minimal lipids

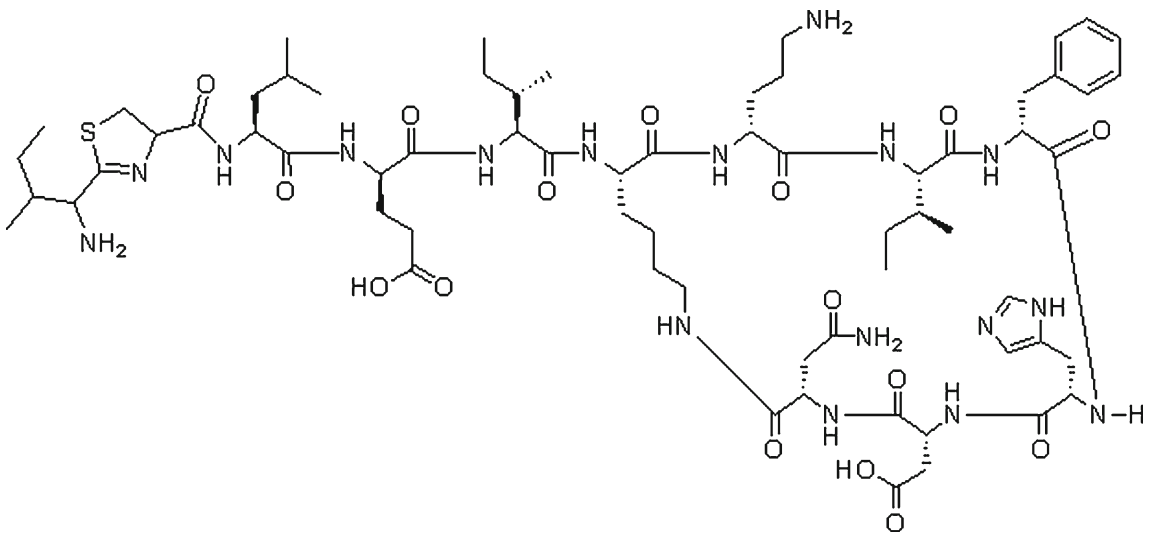

Figure 1. Chemical structure of bacitracin from *Bacillus licheniformis* obtained from the Sigma-Aldrich site, CAS number: 1405-87-4

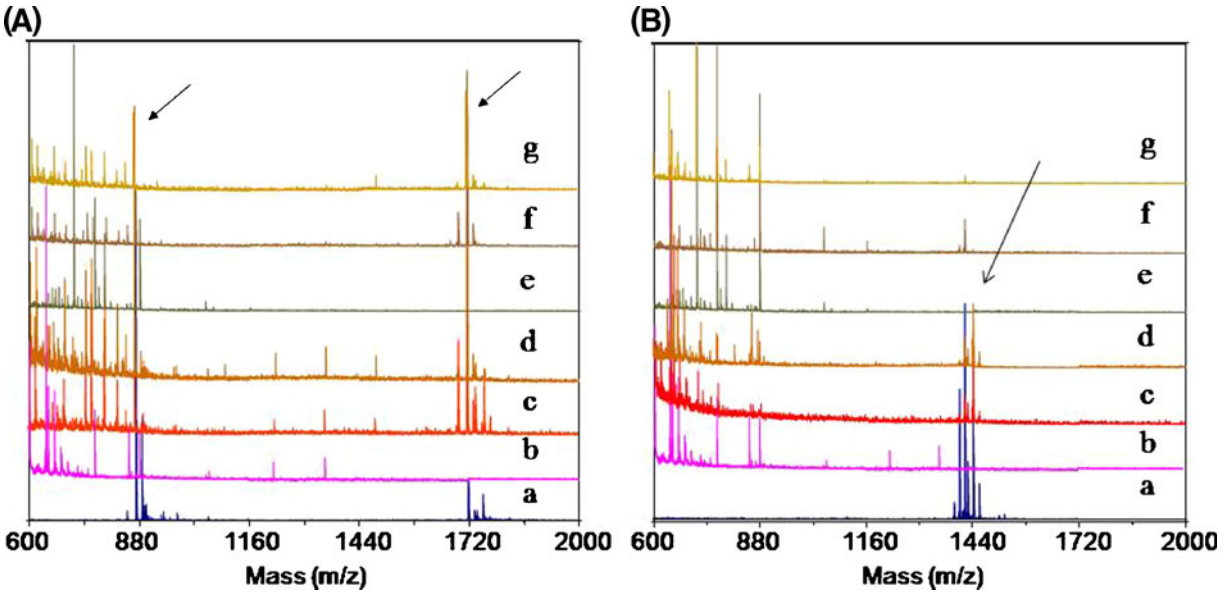

Figure 2. MALDI-TOF-MS analysis of samples extracted from whole cell bacteria after incubation with peptides. Samples obtained from *E. coli* incubated with *amp-1* (**a**, left side) and *amp-2* (**b**, right side). Mass spectrum obtained from only peptides (**a**); only Sample 2 without peptide incubation (**b**); Sample 2 after peptide incubation (100 μM) (**c**); Sample 2 after peptide incubation (40 μM) (**d**); only Sample 1 (**e**); Sample 1 after peptide incubation (100 μM) (**f**); Sample 1 after peptide incubation (40 μM) (**g**). Arrows indicate the peptide ions

amount with an adequate proportion [23]. A Lamarckian genetic algorithm was used as the search method to find the best peptide–membrane complex. Fifty docking runs were done for each peptide with both membranes (Gram-negative and -positive), where the maximum freedom to side chains was unlocked. The generated structures were ranked in two steps: first a cluster with the best models with lowest energy, and second with a root-mean-square deviation (RMSD), for all atoms docked with the membrane, showing tolerance of 4 Å, as recommended for blind docking [25]. The program PyMol [19] http://pymol.sourceforge.net/ was used to characterize peptide-membrane interactions.

Results and Discussion

The emerging incidence of antimicrobial resistance mechanisms developed by microbial pathogens remains a serious challenge to public health worldwide. Opportunistic pathogens such as viruses, fungi, and bacteria can invade various tissues and cause systemic infections, which are considered life-threatening for the patient [26]. Also, the infectious diseases caused by antibiotic-resistant microorganisms have contributed to make the situation worse, especially for those patients whose treatment with currently available drugs has become less efficient [27, 28]. Thus, there is an urgent need for the development of alternative methodologies to help modify this situation.

Here, mass spectrometry technology was used to address the bacterial infection problem focusing on antimicrobial peptides affinity. A method to determine AMPs affinity for bacterial membranes was developed here. First, an *in vitro* initial affinity assay revealed the presence of peptide ions in both Sample 1 (supernatant) and Sample 2 (residual supernatant), with different intensities. The relation observed in peptide signal intensity is directly proportional to an increase in peptide concentration during incubation. Both *amp-1* and *amp-2* were observed in Sample 1 due to their attachment or adherence to bacterial cells. The peptide ions visualized in Sample 2 might be a result of tight attachment or integration into the cell. The maximum signal intensity of *amp-1* is observed for *E. coli* compared with *S. epidermidis*, whereas the signal of *amp-2* is more prominent in *S. epidermidis* than *E. coli* (Figure 2). The

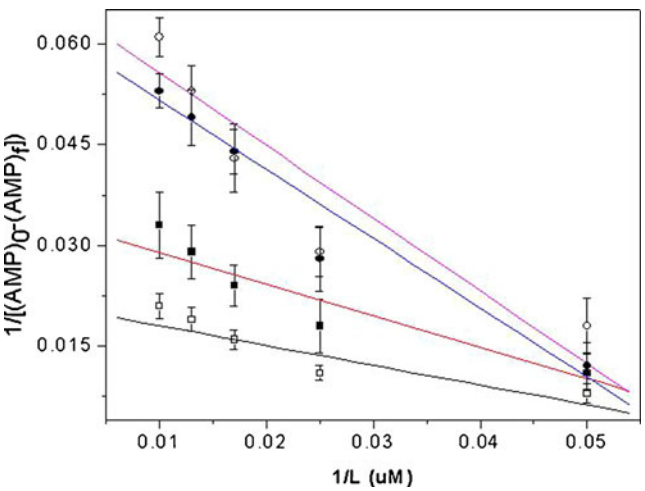

Figure 3. MALDI-TOF-MS equilibration graph showing the relative plot of affinity binding constant. The plot with magenta represents *amp-1* affinity to *E. coli*, red represents *amp-1* affinity to *S. epidermidis*, black represents *amp-2* affinity to *E. coli*, and blue *amp-2* affinity to *S. epidermidis*. Data in each point are the mean of triplicates of individual experiments ± SE

values encountered for the affinity binding constant to *amp-1* were found to be 17.78±0.74 and 14±1.79 μM to *E. coli* and *S. epidermidis*, respectively. Otherwise, for *amp-2,* values of 12.00±1.56 and 18.68±1.45 μM to *E. coli* and *S. epidermidis* were, respectively, found (Figure 3). Affinity binding data showed that *amp-1* has more affinity for the Gram-negative bacterial membrane than for the Gram-positive bacterial membrane. In addition, bacitracin has more affinity for the

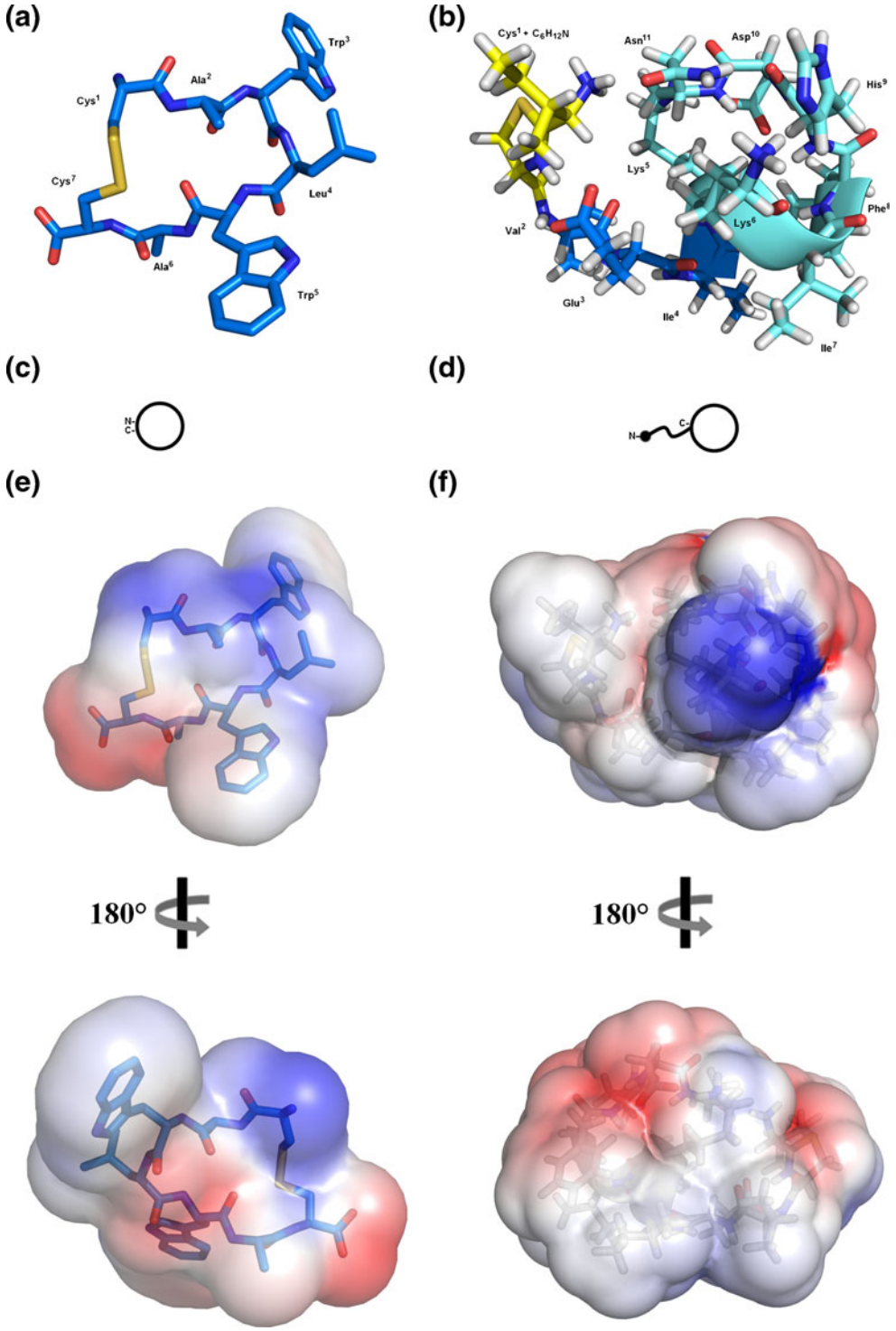

Figure 4. A*mp-1* and *amp-2* three-dimensional models constructed by homology (**a**) and (**b**). (**c**) and (**d**) are schematic representations of both peptides indicating N- and C-terminus locations and modifications represented by * in N-terminus. (**e**) and (**f**) are electrostatic surfaces calculated by ABPS, where blue is positive charge, red is negative charge, and white represents apolar regions. The structures were visualized by PyMol

Gram-positive bacterial membrane, which is in agreement with an earlier report [11].

Thus, the variation of AMP signal intensities provides evidence that AMPs act on bacterial surfaces by either binding to the membrane or by translocation to intracellular targets. Moreover, the data provided insight into the measurement of the binding affinity of AMPs to the bacterial surface, which might be useful to determine their activity. The results indicated that this is a straightforward method for high throughput screening of AMPs to establish their selectivity and binding affinity to the bacterial surface.

In order to evaluate and complement the *in vitro* results, theoretical models of *amp-1* and *amp-2* were constructed and structures were minimized with the YASARA program. A Procheck summary of *amp-1* and *amp-2* showed that for both, 100 % of amino acid residues are located in the most favorable regions in the Ramachandran Plot. Structural differences between the template's structures and predicted three-dimensional structure of the peptide model were calculated by superimposition of backbones onto the template structures. The RMSD values for *amp-1* and *amp-2* between templates and theoretical models were of 1.05 and 2.10 Å, respectively. In addition, the general qualities for the models were reliable in accordance with values –0.58 and –0.21 for the g-factor, respectively. The RMSD values and variability observed among the experimental structure templates and the modeled structure demonstrated a fold modification due to the post-modification carried out in the structure of *amp-1* and *amp-2*. The peptide *amp-1* did not demonstrate any secondary structure. This fact could probably be explained by cyclization and also by the short sequence observed.

In contrast, *amp-2* presented a short α-helix inside the ring after cyclization and addition of the carbonic chain ($C_6H_{12}N$). The *amp-1* model consists of a "symmetric hydrophobic ring," which is linked through disulfide bond formation, between the first and final cysteine amino acid residue (Cys^1-Cys^7). The formation of a "hydrophobic ring" favors the exposure of a hydrophobic amino acid such as Trp^3, Leu^4 and Trp^5 (Figure 4a). The structural modifications of *amp-2* were directed through cyclization involving a covalent link between nitrogen from the side chain (Lys^5) and carbon of the carboxyl group (Asn^{11}) being released H_2O molecule in a hydrolysis reaction as observed in the chemical formula detailed above in methodology session. This cyclization generates an "amphipathic ring-tail peptide" with 36 % of hydrophobic ratio and zero charge for the polypeptide chain (Figure 4c). In addition, the amino acid residues exposed in the "amphipathic ring-tail peptide" were Lys^6 and His^9 on one side and Ile^4, Ile^7 and Phe^8 on the other (Figure 4d).

Furthermore, a correlation between peptide-membrane by *in vitro* and *in silico* was also evaluated in order to better understand the mechanism of action of both peptides. The affinities of amp-*1* and *amp-2* were also analyzed *in silico* against bacterial membranes models. For this, two anionic membranes composed of lipids, DPPE and DPPG were constructed as described in the methodology. The peptides were left close to both membranes (Gram-negative and -positive) allowing random contact by all surfaces. *Amp-1* demonstrated greater affinity for the Gram-negative membrane by *in vitro* assays. This was also corroborated by *in silico* studies comparing the output energy encountered in the well defined cluster generated

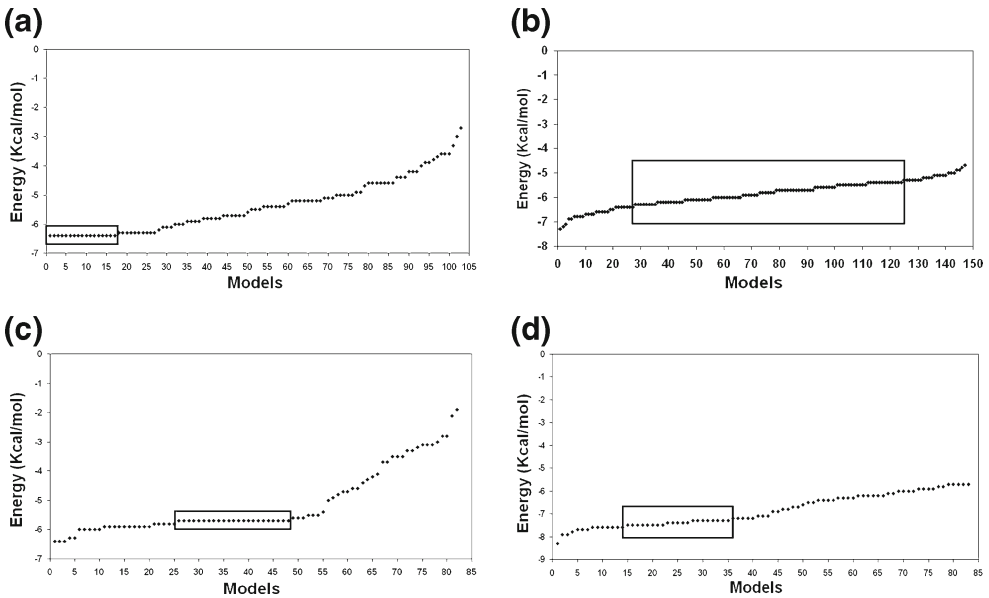

Figure 5. Output results observed after analysis of 50 runs and clusterization in docking studies for *amp-1* and *amp-2*. (**a**) and (**b**) are *amp-1* and *amp-2* outputs of Gram-negative membranes, and (**c**) and (**d**) are *amp-1* and *amp-2* outputs of forward Gram-positive membranes, respectively. Inside square represents the ranked dock cluster. For the *amp-2* models with multiple energies, an average was calculated for both Gram-negative and Gram-positive membrane energy

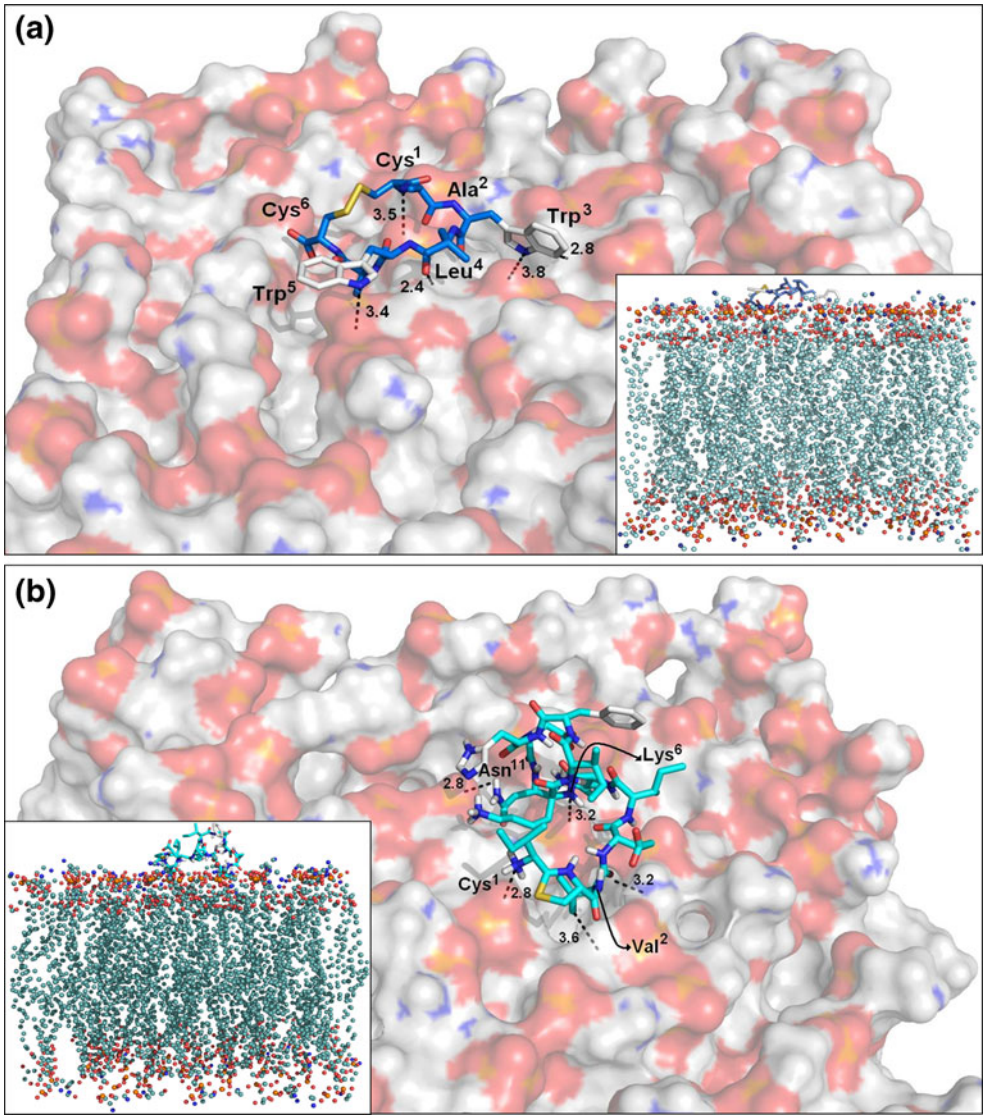

Figure 6. Interaction of (**a**) *amp-1* and (**b**) *amp-2* with Gram-negative membrane in detailed zoom interaction, demonstrating the amino acid residues involved in binding process. Traced lines correspond to non-covalent interactions. Inside square represents a lateral vision of the interaction, demonstrating the complementarity between the peptides and Gram-negative membranes

after data mining observed in both membranes. The energy value observed for *amp-1* toward the Gram-negative membrane was of –6.4 Kcal.mol^{-1}, while the energy observed for *amp-1* forward the Gram-positive membrane was –5.7 Kcal.mol^{-1}, demonstrating a minor interaction affinity (Figure 5c). The *in silico* data also corroborated *amp-2* affinity, reinforcing the *in vitro* assays demonstrating that *amp-2* strongly interacted with the Gram-positive membrane. The output energy observed for *amp-2* and Gram-negative and -positive were –5.8±0.3 and –7.5± 0.1 Kcal.mol^{-1}, respectively, suggesting a clear preference of *amp-2* for Gram-positive membranes (Figure 5d).

Table 1. *In Silico* Interaction Summary Between *amp-1* and Gram-Negative Bacterial Membrane. H Represent Hydrophobic Interaction and HB the Hydrogen Bonds

amp-1			Distance (Å)	Gram-negative			Interaction
Residue	Position	Atom name		Atom name	Position	Phospholipids	
Cys	1	N	3.5	O14	49	DPPG	HB
Trp	3	NE1	3.8	O14	49	DPPG	HB
Trp	3	C	2.8	C11	49	DPPG	HB
Leu	4	O	2.4	N	19	DPPE	HB
Trp	5	NE1	3.2	O14	48	DPPG	HB

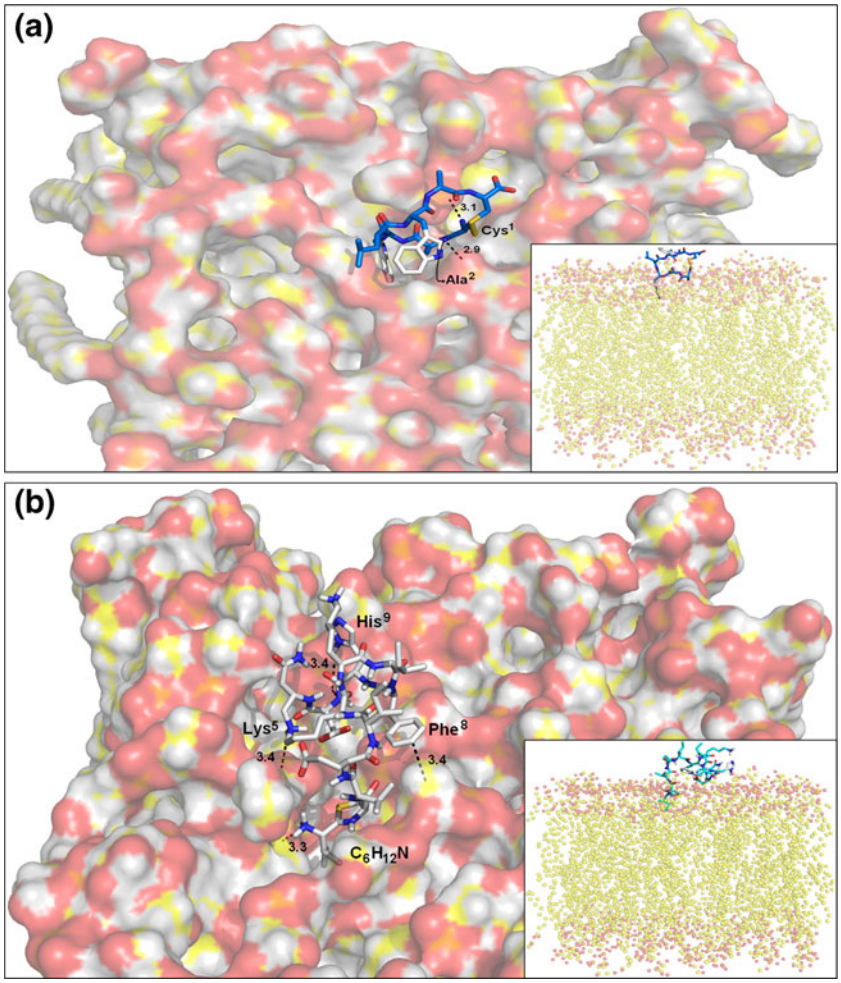

Figure 7. Interaction of (**a**) *amp-1* and (**b**) *amp-2* with Gram-positive membrane in detailed zoom interaction, demonstrating the amino acid residues involved in binding process. Traced lines correspond to non-covalent interactions. Inside square represents a lateral vision of the interaction, demonstrating the complementarity between the peptides and Gram-positive membrane

Docking interaction analysis showed that *amp-1*, which has high hydrophobicity (all amino acid residues were hydrophobic), appeared to be involved in interaction with phospholipid carbons that compose the membrane (Figure 6a). Trp^3, Leu^4, and Trp^5 are the main residues involved, as previously observed for other cyclic peptides such as cyclotides [29]. In this case, it was possible to observe that the mechanism of interaction between parigidin-br1 and DPC micelles has the participation of hydrophobic amino acid residues, such as Phe^7 and Ile^8 in loop 2 and Ile^{11} and Leu^{14} in loop 3. A recent study of kalata B1 and analogs determined that these cyclotides bind specifically to phosphatidylethanolamine [30, 31]. In addition, among the different classes of antimicrobial peptides, the small peptides rich in tryptophan are interestingly studied due to their relative high potency and selectivity. This hydrophobic amino acid has a preference for the interfacial region of the membrane bilayer. In these peptides tryptophan-rich the residue might to function as anchors into the bilayer hydrophobic core and prolongs their attachment to the membrane [32–34]. This information corroborated with data here observed where the tryptophan residues also anchor into bilayer hydrophobic core. The first interaction observed was a hydrogen bond between Cys^1 and $DPPG^{49}$ through N (nitrogen backbone) and O14 (oxygen head group) with distance of 3.5 Å (Table 1). A hydrophobic link

Table 2. *In Silico* Interaction Summary Between *amp-1* and Gram-Positive Bacterial Membrane. HB Represents Hydrogen Bonds

amp-1			Distance (Å)	Gram-positive			Interaction
Residue	Position	Atom name		Atom name	Position	Phospholipids	
Cys	1	N	3.1	O14	47	DPPG	HB
Ala	2	N	2.9	O13	20	DPPG	HB

Table 3. *In Silico* Interaction Summary Between *amp-2* and Gram-Negative Bacterial Membrane. H Represent Hydrophobic Interaction and HB the Hydrogen Bonds

amp-2			Distance (Å)	Gram-negative			Interaction
Residue	Position	Atom name		Atom name	Position	Phospholipids	
Val	2	O	3.2	N	18	DPPE	HB
Val	2	CG2	3.6	C11	49	DPPG	H
Lys	6	N	3.2	O14	19	DPPE	HB
Asn	11	ND2	2.8	O14	49	DPPG	HB
$C_6H_{12}N$	N-termini	N7	2.8	O14	18	DPPE	H

involving carbons was also observed. This interaction probably occurs between aromatic ring carbons of Trp^3 and the apolar carbon chain of phospholipids $DPPG^{49}$ with a distance of 2.8 Å. In addition, the formation of a hydrogen bond was also observed between NE1 (aromatic ring) of Trp^3 and $DPPG^{49}$ through O14 (oxygen head group) with a distance of 3.8 Å. The amino acid residue Leu^4 probably forms a hydrogen bond between O (oxygen backbone) and N (nitrogen head group) of $DPPE^{19}$ with a distance of 2.4 Å. The Trp^5 interacted with $DPPG^{48}$, forming a hydrogen bond between NE1 (aromatic ring) and O14 (oxygen head group) with a distance of 3.2 Å.

In comparison, from the interaction observed between *amp-1* and the Gram-positive membrane (Figure 7a) it was possible to clearly observe that *amp-1* formed only two well defined interactions through backbone nitrogen of Ala^2 and Cys^1 with oxygen atoms (O13 and O14) of $DPPG^{20}$ and $DPPG^{47}$, with a distance of 2.9 and 3.1 Å, respectively, probably indicating a major affinity by Gram-negative membranes (Table 2).

Docking studies revealed that the "hydrophobic tail" at the *amp-2* N-terminus has a key role in membrane interaction (Figure 6b). *Amp-2* demonstrated a hydrogen bond formed between the oxygen backbone (O) in Val^2 and the nitrogen head group (N) of $DPPE^{18}$ from Gram-negative membrane with a distance of 3.2 Å. Another interaction observed involving Val^2 seems to be a hydrophobic interaction between carbon (CG2) and carbon (C11) of $DPPG^{49}$ with a distance of 3.6 Å. The Lys^6 in *amp-2* formed a hydrogen bond between nitrogen backbones (N) with oxygen head group (O14) of $DPPE^{19}$ with a distance of 3.2 Å. The amino acid residue Asn^{11} interacts with head group $DPPG^{49}$, forming a hydrogen interaction between nitrogen (ND2) and oxygen, respectively, with a distance of 2.8 Å. The "hydrophobic tail" added into *amp-2* also showed an interesting property since it probably involved a hydrogen bond formation between nitrogen (N7) of modification and oxygen head group (O14) in $DPPE^{18}$ with a distance of 2.8 Å (Table 3).

In contrast, *amp-2* presented a hydrophobic interaction between the carbons (aromatic ring) Phe^8 and carbon (C13) in $DPPG^{15}$ with a distance of 3.4 Å. Two electrostatic interactions were observed with the participation of nitrogen side chain (NZ and ND1) in Lys^5 and His^9 among oxygen head group (O14) in $DPPG^{46}$ and $DPPG^{47}$, respectively, with a distance of 3.4 Å. In the *amp-2* interaction toward a Gram-positive membrane (Figure 7b) it was possible to identify the insertion into membrane core involving the "hydrophobic tail" ($C_6H_{12}N$). This insertion is probably firstly guided through hydrogen bond formation between nitrogen (N7) and oxygen head group of phospholipids $DPPE^{18}$ with a distance around 3.3 Å. Probably hydrophobic interactions inside the core might be formed with the insertion of the "hydrophobic tail", since the distance observed was less than 3.5 Å (Table 4). The *in silico* studies showed that an *amp-2* interacts more energetically toward a Gram-positive membrane and this might be reinforced by formation of a hydrogen bond, and by electrostatic and mainly hydrophobic interactions.

Conclusion

The *in vitro* assays indicated that *amp-1* has slightly more affinity to *E. coli* and *amp-2* has higher affinity to *S. epidermidis*. Interestingly, *amp-1* showed both monomer and dimer ions in mass spectrometry analysis. Earlier, Glukhov and coworkers [5] established that dimerization or oligomerization of peptides enhanced the antimicrobial

Table 4. *In Silico* Interaction Summary Between *amp-2* and Gram-Positive Bacterial Membrane. H Represents Hydrophobic Interactions and EI the Electrostatic Interaction

amp-2			Distance (Å)	Gram-positive			Interaction
Residue	Position	Atom name		Atom name	Position	Phospholipids	
Phe	8	C	3.4	C13	15	DPPG	H
Lys	5	NZ	3.4	O14	47	DPPG	EI
His	9	ND1	3.4	C11	49	DPPG	EI
$C_6H_{12}N$	N-termini	N7	3.3	O	18	DPPE	HB
$C_6H_{12}N$	N-termini	C	–	C	Pocket	DPPG19/20/47	H

activity. The initial ion intensities of *amp-1* and *amp-2* were obtained at 100 μM peptide concentration. The intensities of different concentration peptides incubated with bacterial cells varied significantly, but the ions coming from the bacterium itself remained unchanged. Both monomer and dimer ions of *amp-1* were considered for affinity binding calculations. Bacterial membranes strongly bind peptide dimers onto their surface by "sinking" of the hydrophobic core segment into the membrane. The equilibrium concentration of the antimicrobial peptides can be derived from the peak intensities in the mass spectra using the double reciprocal plot [35, 36] and the affinity binding constant (K). After *in silico* assays it was possible to conclude that amp-1 and amp-2 interestingly corroborated *in vitro* data, reinforcing the idea of affinity and helping to understand the possible interaction mode. Data here provided show that it is possible to combine theoretical and practical analyses to help solve the problems of infectious disease.

Acknowledgments

The authors acknowledge support for this work by CAPES, CNPq, FAPDF, and UCB.

References

1. Maria-Neto, S., Cândido, E.S., Rodrigues, D.R., de Sousa, D.A., da Silva, E.M., de Moraes, L.M., Otero-Gonzalez, A.J., Magalhães, B.S., Dias, S.C., Franco, O.L.: Deciphering the magainin resistance process of *Escherichia coli* strains in light of the cytosolic proteome. *Antimicrob. Agents Chemother.* **56**, 1714–1724 (2012)
2. Andra, J., Monreal, D., Martinez de Tejada, G., Olak, C., Brezesinski, G., Gomez, S.S., Goldmann, T., Bartels, R., Brandenburg, K., Moriyon, I.: Rationale for the design of shortened derivatives of the NK-lysin-derived antimicrobial peptide NK-2 with improved activity against Gram-negative pathogens. *J. Biol. Chem.* **282**, 14719–14728 (2007)
3. Mandal, S.M., Dey, S., Mandal, M., Sarkar, S., Maria-Neto, S., Franco, O.L.: Identification and structural insights of three novel antimicrobial peptides isolated from green coconut water. *Peptides* **30**, 633–637 (2009)
4. Mechler, A., Praporski, S., Atmuri, K., Boland, M., Separovic, F., Martin, L.L.: Specific and selective peptide–membrane interactions revealed using quartz crystal microbalance. *Biophys. J.* **93**, 3907–3916 (2007)
5. Glukhov, E., Stark, M., Burrows, L.L., Deber, C.M.: Basis for selectivity of cationic antimicrobial peptides for bacterial versus mammalian membranes. *J. Biol. Chem.* **280**, 33960–33967 (2005)
6. Fernandez, D.I., Gehman, J.D., Separovic, F.: Membrane interactions of antimicrobial peptides from Australian frogs. *Biochim. Biophys. Acta* **1788**, 1630–1638 (2009)
7. van de Kerk-van Hoof, A., Heck, A.J.: Interactions of alpha- and beta-avoparcin with bacterial cell-wall receptor-mimicking peptides studied by electrospray ionization mass spectrometry. *J. Antimicrob. Chemother.* **44**, 593–599 (1999)
8. Mandal, S.M., Pati, B.R., Ghosh, A.K., Das, A.K.: Letter: Influence of experimental parameters on identification of whole cell Rhizobium by matrix-assisted laser desorption/ionization time-of-flight mass spectrometry. *Eur. J. Mass Spectrom. (Chichester, Eng)* **13**, 165–171 (2007)
9. Schibli, D.J., Epand, R.F., Vogel, H.J., Epand, R.M.: Tryptophan-rich antimicrobial peptides: Comparative properties and membrane interactions. *Biochem. Cell Biol.* **80**, 667–677 (2002)
10. Mandal, S.M., Migliolo, L., Franco, O.L., Ghosh, A.K.: Identification of an antifungal peptide from *Trapa natans* fruits with inhibitory effects on *Candida tropicalis* biofilm formation. *Peptides* **32**, 1741–1747 (2011)
11. Sleytr, U.B., Oliver, T.C., Thorne, K.J.: Bacitracin-induced changes in bacterial plasma membrane structure. *Biochim. Biophys. Acta* **419**, 570–573 (1976)
12. Chan, W.C., White, P.D.: Fmoc solid phase peptide synthesis: a practical approach. Oxford University Press: Oxford, U. K. p 346 (2000)
13. Murphy, J., Kies, M.: Note on the spectrophotometric determination of proteins in dilute solutions. *Biochim. Biophys. Acta* **45**, 382–384 (1960)
14. Nicastro, G., Franzoni, L., de Chiara, C., Mancin, A.C., Giglio, J.R., Spisni, A.: Solution structure of crotamine, a Na^+ channel affecting toxin from *Crotalus durissus* terrificus venom. *Eur. J. Biochem.* **270**, 1969–1979 (2003)
15. Wei, Y., Kim, S., Fela, D., Baum, J., Hecht, M.H.: Solution structure of a de novo protein from a designed combinatorial library. *Proc. Natl. Acad. Sci. U. S. A.* **100**, 13270–13273 (2003)
16. Eswar, N., Webb, B., Marti-Renom, M.A., Madhusudhan, M.S., Eramian, D., Shen, M.Y., Pieper, U., Sali, A.: Comparative protein structure modeling using Modeller. *Curr. Protoc. Bioinforma.* **5**, Units 5–6 (2006)
17. Wiederstein, M., Sippl, M.J.: ProSA-web: Interactive web service for the recognition of errors in three-dimensional structures of proteins. *Nucleic Acids Res.* **35**, W407–W410 (2007)
18. Sumathi, K., Ananthalakshmi, P., Roshan, M.N., Sekar, K.: 3dSS: 3D structural superposition. *Nucleic Acids Res.* **34**, W128–W132 (2006)
19. DeLano, W.: The PyMOL molecular graphics system. De Lano Scientific, San Carlos, C. A. (2002)
20. Wilkins, M.R., Gasteiger, E., Bairoch, A., Sanchez, J.C., Williams, K.L., Appel, R.D., Hochstrasser, D.F.: Protein identification and analysis tools in the ExPASy server. *Methods Mol. Biol.* **112**, 531–552 (1999)
21. Sousa, S.F., Fernandes, P.A., Ramos, M.J.: Protein-ligand docking: Current status and future challenges. *Proteins* **65**, 15–26 (2006)
22. Jo, S., Lim, J.B., Klauda, J.B., Im, W.: CHARMM-GUI Membrane Builder for mixed bilayers and its application to yeast membranes. *Biophys. J.* **97**, 50–58 (2009)
23. Lohner, K., Sevcsik, E., Pabst, G.: Liposome-Based Biomembrane Mimetic Systems: Implications for Lipid–Peptide Interactions, Vol. 6. Advances in Planar Lipid Bilayers and Liposomes. Elsevier Inc., Austria (2008)
24. Pimthon, J., Willumeit, R., Lendlein, A., Hofmann, D.: Membrane association and selectivity of the antimicrobial peptide NK-2: A molecular dynamics simulation study. *J. Pept. Sci.* **15**, 654–667 (2009)
25. Jitonnom, J., Lomthaisong, K., Lee, V.S.: Computational design of peptide inhibitor based on modifications of proregion from *Plutella xylostella* midgut trypsin. *Chem. Biol. Drug Des.* **79**, 583–593 (2012)
26. Cutler, D.M.: The lifetime costs and benefits of medical technology. *J. Health Econ.* **26**, 1081–1100 (2007)
27. Foubister, V.: New mode of intervention in sepsis treatment. *Drug Discov. Today* **8**, 610–612 (2003)
28. Carrillo-Munoz, A.J., Giusiano, G., Ezkurra, P.A., Quindos, G.: Antifungal agents: Mode of action in yeast cells. *Rev. Esp. Quimioter.* **19**, 130–139 (2006)
29. Pinto, M.F., Fensterseifer, I.C., Migliolo, L., Sousa, D.A., de Capdville, G., Arboleda-Valencia, J.W., Colgrave, M.L., Craik, D.J., Magalhaes, B.S., Dias, S.C., Franco, O.L.: Identification and structural characterization of novel cyclotide with activity against an insect pest of sugar cane. *J. Biol. Chem.* **287**, 134–147 (2012)
30. Lee, C.C., Sun, Y., Qian, S., Huang, H.W.: Transmembrane pores formed by human antimicrobial peptide LL-37. *Biophys. J.* **100**, 1688–1696 (2011)
31. Subramanian, S., Ross, N.W., MacKinnon, S.L.: Myxinidin, a novel antimicrobial peptide from the epidermal mucus of hagfish, Myxine glutinosa L. *Mar. Biotechnol. (NY)* **11**, 748–757 (2009)
32. Chan, D.I., Prenner, E.J., Vogel, H.J.: Tryptophan- and arginine-rich antimicrobial peptides: Structures and mechanisms of action. *Biochim. Biophys. Acta* **1758**, 1184–1202 (2006)
33. Rezansoff, A.J., Hunter, H.N., Jing, W., Park, I.Y., Kim, S.C., Vogel, H.J.: Interactions of the antimicrobial peptide Ac-FRWWHR-NH(2) with model membrane systems and bacterial cells. *J. Peptide Res.* **65**, 491–501 (2005)
34. de Planque, M.R., Bonev, B.B., Demmers, J.A., Greathouse, D.V., Koeppe II, R.E., Separovic, F., Watts, A., Killian, J.A.: Interfacial anchor properties of tryptophan residues in transmembrane peptides can dominate over hydrophobic matching effects in peptide–lipid interactions. *Biochemistry* **42**, 5341–5348 (2003)
35. Klotz, I.M., Hunston, D.L.: Properties of graphical representations of multiple classes of binding sites. *Biochemistry* **10**, 3065–3069 (1971)
36. Nafisi, S., Sobhanmanesh, A., Alimoghaddam, K., Ghavamzadeh, A., Tajmir-Riahi, H.A.: Interaction of arsenic trioxide As2O3 with DNA and RNA. *DNA Cell Biol.* **24**, 634–640 (2005)